Updated Measurement of the Single Top Quark Production Cross Section and |Vtb| in the Missing Transverse Energy Plus Jets Topology in $p\bar{p}$ Collisions at $\sqrt{s} = 1.96$ TeV

CDF Collaboration ; et al ; Canelli, F ; Kilminster, B

Abstract: An updated measurement of the single top quark production cross section is presented using the full data set collected by the Collider Detector at Fermilab (CDF), corresponding to 9.5 fb-1 of integrated luminosity from proton-antiproton collisions at 1.96 TeV center-of-mass energy. The events selected contain an imbalance in the total transverse momentum, jets identified as containing b quarks, and no identified leptons. The sum of the s- and t-channel single top quark cross sections is measured to be 3.53-1.16+1.25 pb and a lower limit on the magnitude of the top-to-bottom quark coupling, |Vtb| of 0.63, is obtained at the 95% credibility level. These measurements are combined with previously reported CDF results obtained from events with an imbalance in total transverse momentum, jets identified as originating from b quarks, and one identified lepton. The combined cross section is measured to be 3.02-0.48+0.49 pb and a lower limit on |Vtb| of 0.84 is obtained at the 95% credibility level.

Updated Measurement of the Single Top Quark Production Cross Section and $|V_{tb}|$ in the Missing Transverse Energy Plus Jets Topology in $p\bar{p}$ Collisions at $\sqrt{s} = 1.96$ TeV

T. Aaltonen,[21] S. Amerio[jj],[39] D. Amidei,[31] A. Anastassov[v],[15] A. Annovi,[17] J. Antos,[12] G. Apollinari,[15] J.A. Appel,[15] T. Arisawa,[52] A. Artikov,[13] J. Asaadi,[47] W. Ashmanskas,[15] B. Auerbach,[2] A. Aurisano,[47] F. Azfar,[38] W. Badgett,[15] T. Bae,[25] A. Barbaro-Galtieri,[26] V.E. Barnes,[43] B.A. Barnett,[23] P. Barria[ll],[41] P. Bartos,[12] M. Bauce[jj],[39] F. Bedeschi,[41] S. Behari,[15] G. Bellettini[kk],[41] J. Bellinger,[54] D. Benjamin,[14] A. Beretvas,[15] A. Bhatti,[45] K.R. Bland,[5] B. Blumenfeld,[23] A. Bocci,[14] A. Bodek,[44] D. Bortoletto,[43] J. Boudreau,[42] A. Boveia,[11] L. Brigliadori[ii],[6] C. Bromberg,[32] E. Brucken,[21] J. Budagov,[13] H.S. Budd,[44] K. Burkett,[15] G. Busetto[jj],[39] P. Bussey,[19] P. Butti[kk],[41] A. Buzatu,[19] A. Calamba,[10] S. Camarda,[4] M. Campanelli,[28] F. Canelli[cc],[11] B. Carls,[22] D. Carlsmith,[54] R. Carosi,[41] S. Carrillo[l],[16] B. Casal[j],[9] M. Casarsa,[48] A. Castro[ii],[6] P. Catastini,[20] D. Cauz[qqrr],[48] V. Cavaliere,[22] A. Cerri[e],[26] L. Cerrito[q],[28] Y.C. Chen,[1] M. Chertok,[7] G. Chiarelli,[41] G. Chlachidze,[15] K. Cho,[25] D. Chokheli,[13] A. Clark,[18] C. Clarke,[53] M.E. Convery,[15] J. Conway,[7] M. Corbo[y],[15] M. Cordelli,[17] C.A. Cox,[7] D.J. Cox,[7] M. Cremonesi,[41] D. Cruz,[47] J. Cuevas[x],[9] R. Culbertson,[15] N. d'Ascenzo[u],[15] M. Datta[ff],[15] P. de Barbaro,[44] L. Demortier,[45] M. Deninno,[6] M. D'Errico[jj],[39] F. Devoto,[21] A. Di Canto[kk],[41] B. Di Ruzza[p],[15] J.R. Dittmann,[5] S. Donati[kk],[41] M. D'Onofrio,[27] M. Dorigo[ss],[48] A. Driutti[qqrr],[48] K. Ebina,[52] R. Edgar,[31] A. Elagin,[47] R. Erbacher,[7] S. Errede,[22] B. Esham,[22] S. Farrington,[38] J.P. Fernández Ramos,[29] R. Field,[16] G. Flanagan[s],[15] R. Forrest,[7] M. Franklin,[20] J.C. Freeman,[15] H. Frisch,[11] Y. Funakoshi,[52] C. Galloni[kk],[41] A.F. Garfinkel,[43] P. Garosi[ll],[41] H. Gerberich,[22] E. Gerchtein,[15] S. Giagu,[46] V. Giakoumopoulou,[3] K. Gibson,[42] C.M. Ginsburg,[15] N. Giokaris,[3] P. Giromini,[17] V. Glagolev,[13] D. Glenzinski,[15] M. Gold,[34] D. Goldin,[47] A. Golossanov,[15] G. Gomez,[9] G. Gomez-Ceballos,[30] M. Goncharov,[30] O. González López,[29] I. Gorelov,[34] A.T. Goshaw,[14] K. Goulianos,[45] E. Gramellini,[6] C. Grosso-Pilcher,[11] R.C. Group,[51,15] J. Guimaraes da Costa,[20] S.R. Hahn,[15] J.Y. Han,[44] F. Happacher,[17] K. Hara,[49] M. Hare,[50] R.F. Harr,[53] T. Harrington-Taber[m],[15] K. Hatakeyama,[5] C. Hays,[38] J. Heinrich,[40] M. Herndon,[54] A. Hocker,[15] Z. Hong,[47] W. Hopkins[f],[15] S. Hou,[1] R.E. Hughes,[35] U. Husemann,[55] M. Hussein[aa],[32] J. Huston,[32] G. Introzzi[nnoo],[41] M. Iori[pp],[46] A. Ivanov[o],[7] E. James,[15] D. Jang,[10] B. Jayatilaka,[15] E.J. Jeon,[25] S. Jindariani,[15] M. Jones,[43] K.K. Joo,[25] S.Y. Jun,[10] T.R. Junk,[15] M. Kambeitz,[24] T. Kamon,[25,47] P.E. Karchin,[53] A. Kasmi,[5] Y. Kato[n],[37] W. Ketchum[gg],[11] J. Keung,[40] B. Kilminster[cc],[15] D.H. Kim,[25] H.S. Kim,[25] J.E. Kim,[25] M.J. Kim,[17] S.H. Kim,[49] S.B. Kim,[25] Y.J. Kim,[25] Y.K. Kim,[11] N. Kimura,[52] M. Kirby,[15] K. Knoepfel,[15] K. Kondo,[52,*] D.J. Kong,[25] J. Konigsberg,[16] A.V. Kotwal,[14] M. Kreps,[24] J. Kroll,[40] M. Kruse,[14] T. Kuhr,[24] M. Kurata,[49] A.T. Laasanen,[43] S. Lammel,[15] M. Lancaster,[28] K. Lannon[w],[35] G. Latino[ll],[41] H.S. Lee,[25] J.S. Lee,[25] S. Leo,[41] S. Leone,[41] J.D. Lewis,[15] A. Limosani[r],[14] E. Lipeles,[40] A. Lister[a],[18] H. Liu,[51] Q. Liu,[43] T. Liu,[15] S. Lockwitz,[55] A. Loginov,[55] D. Lucchesi[jj],[39] A. Lucà,[17] J. Lueck,[24] P. Lujan,[26] P. Lukens,[15] G. Lungu,[45] J. Lys,[26] R. Lysak[d],[12] R. Madrak,[15] P. Maestro[ll],[41] S. Malik,[45] G. Manca[b],[27] A. Manousakis-Katsikakis,[3] L. Marchese[hh],[6] F. Margaroli,[46] P. Marino[mm],[41] K. Matera,[22] M.E. Mattson,[53] A. Mazzacane,[15] P. Mazzanti,[6] R. McNulty[i],[27] A. Mehta,[27] P. Mehtala,[21] C. Mesropian,[45] T. Miao,[15] D. Mietlicki,[31] A. Mitra,[1] H. Miyake,[49] S. Moed,[15] N. Moggi,[6] C.S. Moon[y],[15] R. Moore[ddee],[15] M.J. Morello[mm],[41] A. Mukherjee,[15] Th. Muller,[24] P. Murat,[15] M. Mussini[ii],[6] J. Nachtman[m],[15] Y. Nagai,[49] J. Naganoma,[52] I. Nakano,[36] A. Napier,[50] J. Nett,[47] C. Neu,[51] T. Nigmanov,[42] L. Nodulman,[2] S.Y. Noh,[25] O. Norniella,[22] L. Oakes,[38] S.H. Oh,[14] Y.D. Oh,[25] I. Oksuzian,[51] T. Okusawa,[37] R. Orava,[21] L. Ortolan,[4] C. Pagliarone,[48] E. Palencia[e],[9] P. Palni,[34] V. Papadimitriou,[15] W. Parker,[54] G. Pauletta[qqrr],[48] M. Paulini,[10] C. Paus,[30] T.J. Phillips,[14] E. Pianori,[40] J. Pilot,[7] K. Pitts,[22] C. Plager,[8] L. Pondrom,[54] S. Poprocki[f],[15] K. Potamianos,[26] A. Pranko,[26] F. Prokoshin[z],[13] F. Ptohos[g],[17] G. Punzi[kk],[41] I. Redondo Fernández,[29] P. Renton,[38] M. Rescigno,[46] F. Rimondi,[6,*] L. Ristori,[41,15] A. Robson,[19] T. Rodriguez,[40] S. Rolli[h],[50] M. Ronzani[kk],[41] R. Roser,[15] J.L. Rosner,[11] F. Ruffini[ll],[41] A. Ruiz,[9] J. Russ,[10] V. Rusu,[15] W.K. Sakumoto,[44] Y. Sakurai,[52] L. Santi[qqrr],[48] K. Sato,[49] V. Saveliev[u],[15] A. Savoy-Navarro[y],[15] P. Schlabach,[15] E.E. Schmidt,[15] T. Schwarz,[31] L. Scodellaro,[9] F. Scuri,[41] S. Seidel,[34] Y. Seiya,[37] A. Semenov,[13] F. Sforza[kk],[41] S.Z. Shalhout,[7] T. Shears,[27] P.F. Shepard,[42] M. Shimojima[t],[49] M. Shochet,[11] I. Shreyber-Tecker,[33] A. Simonenko,[13] K. Sliwa,[50] J.R. Smith,[7] F.D. Snider,[15] H. Song,[42] V. Sorin,[4] R. St. Denis,[19,*] M. Stancari,[15] D. Stentz[v],[15] J. Strologas,[34] Y. Sudo,[49] A. Sukhanov,[15] I. Suslov,[13] K. Takemasa,[49] Y. Takeuchi,[49] J. Tang,[11] M. Tecchio,[31] P.K. Teng,[1] J. Thom[f],[15] E. Thomson,[40] V. Thukral,[47] D. Toback,[47] S. Tokar,[12] K. Tollefson,[32] T. Tomura,[49] D. Tonelli[e],[15] S. Torre,[17] D. Torretta,[15] P. Totaro,[39] M. Trovato[mm],[41] F. Ukegawa,[49] S. Uozumi,[25] F. Vázquez[l],[16] G. Velev,[15] C. Vellidis,[15]

C. Vernieri[mm],[41] M. Vidal,[43] R. Vilar,[9] J. Vizán[bb],[9] M. Vogel,[34] G. Volpi,[17] P. Wagner,[40] R. Wallny[j],[15] S.M. Wang,[1] D. Waters,[28] W.C. Wester III,[15] D. Whiteson[c],[40] A.B. Wicklund,[2] S. Wilbur,[7] H.H. Williams,[40] J.S. Wilson,[31] P. Wilson,[15] B.L. Winer,[35] P. Wittich[f],[15] S. Wolbers,[15] H. Wolfe,[35] T. Wright,[31] X. Wu,[18] Z. Wu,[5] K. Yamamoto,[37] D. Yamato,[37] T. Yang,[15] U.K. Yang,[25] Y.C. Yang,[25] W.-M. Yao,[26] G.P. Yeh,[15] K. Yi[m],[15] J. Yoh,[15] K. Yorita,[52] T. Yoshida[k],[37] G.B. Yu,[14] I. Yu,[25] A.M. Zanetti,[48] Y. Zeng,[14] C. Zhou,[14] and S. Zucchelli[ii]6

(CDF Collaboration)[†]

[1] *Institute of Physics, Academia Sinica, Taipei, Taiwan 11529, Republic of China*
[2] *Argonne National Laboratory, Argonne, Illinois 60439, USA*
[3] *University of Athens, 157 71 Athens, Greece*
[4] *Institut de Fisica d'Altes Energies, ICREA, Universitat Autonoma de Barcelona, E-08193, Bellaterra (Barcelona), Spain*
[5] *Baylor University, Waco, Texas 76798, USA*
[6] *Istituto Nazionale di Fisica Nucleare Bologna, [ii] University of Bologna, I-40127 Bologna, Italy*
[7] *University of California, Davis, Davis, California 95616, USA*
[8] *University of California, Los Angeles, Los Angeles, California 90024, USA*
[9] *Instituto de Fisica de Cantabria, CSIC-University of Cantabria, 39005 Santander, Spain*
[10] *Carnegie Mellon University, Pittsburgh, Pennsylvania 15213, USA*
[11] *Enrico Fermi Institute, University of Chicago, Chicago, Illinois 60637, USA*
[12] *Comenius University, 842 48 Bratislava, Slovakia; Institute of Experimental Physics, 040 01 Kosice, Slovakia*
[13] *Joint Institute for Nuclear Research, RU-141980 Dubna, Russia*
[14] *Duke University, Durham, North Carolina 27708, USA*
[15] *Fermi National Accelerator Laboratory, Batavia, Illinois 60510, USA*
[16] *University of Florida, Gainesville, Florida 32611, USA*
[17] *Laboratori Nazionali di Frascati, Istituto Nazionale di Fisica Nucleare, I-00044 Frascati, Italy*
[18] *University of Geneva, CH-1211 Geneva 4, Switzerland*
[19] *Glasgow University, Glasgow G12 8QQ, United Kingdom*
[20] *Harvard University, Cambridge, Massachusetts 02138, USA*
[21] *Division of High Energy Physics, Department of Physics, University of Helsinki, FIN-00014, Helsinki, Finland; Helsinki Institute of Physics, FIN-00014, Helsinki, Finland*
[22] *University of Illinois, Urbana, Illinois 61801, USA*
[23] *The Johns Hopkins University, Baltimore, Maryland 21218, USA*
[24] *Institut für Experimentelle Kernphysik, Karlsruhe Institute of Technology, D-76131 Karlsruhe, Germany*
[25] *Center for High Energy Physics: Kyungpook National University, Daegu 702-701, Korea; Seoul National University, Seoul 151-742, Korea; Sungkyunkwan University, Suwon 440-746, Korea; Korea Institute of Science and Technology Information, Daejeon 305-806, Korea; Chonnam National University, Gwangju 500-757, Korea; Chonbuk National University, Jeonju 561-756, Korea; Ewha Womans University, Seoul, 120-750, Korea*
[26] *Ernest Orlando Lawrence Berkeley National Laboratory, Berkeley, California 94720, USA*
[27] *University of Liverpool, Liverpool L69 7ZE, United Kingdom*
[28] *University College London, London WC1E 6BT, United Kingdom*
[29] *Centro de Investigaciones Energeticas Medioambientales y Tecnologicas, E-28040 Madrid, Spain*
[30] *Massachusetts Institute of Technology, Cambridge, Massachusetts 02139, USA*
[31] *University of Michigan, Ann Arbor, Michigan 48109, USA*
[32] *Michigan State University, East Lansing, Michigan 48824, USA*
[33] *Institution for Theoretical and Experimental Physics, ITEP, Moscow 117259, Russia*
[34] *University of New Mexico, Albuquerque, New Mexico 87131, USA*
[35] *The Ohio State University, Columbus, Ohio 43210, USA*
[36] *Okayama University, Okayama 700-8530, Japan*
[37] *Osaka City University, Osaka 558-8585, Japan*
[38] *University of Oxford, Oxford OX1 3RH, United Kingdom*
[39] *Istituto Nazionale di Fisica Nucleare, Sezione di Padova, [jj] University of Padova, I-35131 Padova, Italy*
[40] *University of Pennsylvania, Philadelphia, Pennsylvania 19104, USA*
[41] *Istituto Nazionale di Fisica Nucleare Pisa, [kk] University of Pisa, [ll] University of Siena, [mm] Scuola Normale Superiore, I-56127 Pisa, Italy, [nn] INFN Pavia, I-27100 Pavia, Italy, [oo] University of Pavia, I-27100 Pavia, Italy*
[42] *University of Pittsburgh, Pittsburgh, Pennsylvania 15260, USA*
[43] *Purdue University, West Lafayette, Indiana 47907, USA*
[44] *University of Rochester, Rochester, New York 14627, USA*
[45] *The Rockefeller University, New York, New York 10065, USA*

[46] Istituto Nazionale di Fisica Nucleare, Sezione di Roma 1,
[pp] Sapienza Università di Roma, I-00185 Roma, Italy
[47] Mitchell Institute for Fundamental Physics and Astronomy,
Texas A&M University, College Station, Texas 77843, USA
[48] Istituto Nazionale di Fisica Nucleare Trieste, [qq] Gruppo Collegato di Udine,
[rr] University of Udine, I-33100 Udine, Italy, [ss] University of Trieste, I-34127 Trieste, Italy
[49] University of Tsukuba, Tsukuba, Ibaraki 305, Japan
[50] Tufts University, Medford, Massachusetts 02155, USA
[51] University of Virginia, Charlottesville, Virginia 22906, USA
[52] Waseda University, Tokyo 169, Japan
[53] Wayne State University, Detroit, Michigan 48201, USA
[54] University of Wisconsin, Madison, Wisconsin 53706, USA
[55] Yale University, New Haven, Connecticut 06520, USA

(Dated: October 23, 2014)

An updated measurement of the single top quark production cross section is presented using the full data set collected by the Collider Detector at Fermilab (CDF) and corresponding to 9.5 fb^{-1} of integrated luminosity from proton-antiproton collisions at 1.96 TeV center-of-mass energy. The events selected contain an imbalance in the total transverse energy, jets identified as originating from b quarks, and no identified leptons. The sum of the s- and t-channel single top quark cross sections is measured to be $3.53^{+1.25}_{-1.16}$ pb and a lower limit on $|V_{tb}|$ of 0.63 is obtained at the 95% credibility level. These measurements are combined with previously reported CDF results obtained from events with an imbalance in total transverse energy, jets identified as originating from b quarks, and exactly one identified lepton. The combined cross section is measured to be $3.02^{+0.49}_{-0.48}$ pb and a lower limit on $|V_{tb}|$ of 0.84 is obtained at the 95% credibility level.

PACS numbers: 14.65.Ha, 13.85.Ni, 12.15.Hh

The observation of single top quark production at the Tevatron was a significant achievement, allowing measurements of the cross section at a hadron collider [1] and improved bounds on the Cabibbo-Kobayashi-Maskawa (CKM) [2] matrix element magnitude $|V_{tb}|$ due to the direct coupling of the b quark with the singly produced top quark.

For single top quark production, a t-$\bar{b}$ pair is produced through a virtual W^+ boson [3] in either the s or t channel. The top quark subsequently decays to a W^+ boson and a bottom quark, and the fragmentations of the b and $\bar{b}$ quarks result in two jets that can be reconstructed in the detector. For the t-channel process, jets tend to be more boosted along the proton-antiproton beam axis than those originating from the s-channel process; some of these jets are thus emitted in regions that are not instrumented and therefore escape the detector acceptance.

Excluding the contribution from the tW production mode, which is expected to be negligible in the final state considered in this Letter [4], the standard model (SM) prediction for the combined s- and t-channel single top quark production cross section $\sigma^{s+t}_{\rm SM}$ is 3.15 ± 0.36 pb, which has been calculated including next-to-next-to-leading order corrections [5, 6]. The primary sensitivity to measuring this quantity is usually obtained from events where the W boson from the $t \to Wb$ process [7] decays leptonically to a charged lepton ℓ (where ℓ represents either an electron e or muon μ) and an antineutrino, with a pair of jets, one of which is "b-tagged" or identified as likely having originated from a bottom quark. This sample of events (hereafter the "$\ell\nu b\bar{b}$" sample) provides a distinctive signature against backgrounds produced by the strong interaction (QCD multijet or "MJ" background), which contain no leptons and multiple jets.

A complementary approach consists in using final states that contain two or three jets and significant imbalance in the total transverse energy $\not\!\!E_T$ [8], which results from the leptonic decay of the W boson, where the lepton is not identified due to reconstruction or acceptance effects and the neutrino carries significant unmeasured momentum. Although MJ events comprise the dominant background in this final state (hereafter the "$\not\!\!E_T b\bar{b}$" analysis or sample), the requirement of significant $\not\!\!E_T$ greatly suppresses such background. In addition, this search has sensitivity to events where the W boson decays via $W^- \to \tau^-\bar{\nu}_\tau$, and the τ^- decays hadronically, resulting in a reconstructed jet signature.

The first CDF measurement of single top quark production in the $\not\!\!E_T b\bar{b}$ final state was performed with a data set corresponding to an integrated luminosity of 2.1 fb^{-1} [9]. This article presents a new measurement using the full CDF data set (9.5 fb^{-1}). All the techniques developed in the search for s-channel single top quark production in the $\not\!\!E_T b\bar{b}$ sample [10] are exploited in this update. Important aspects of the analysis methodology are restated here for completeness. The results of this analysis and those of the most recent $\ell\nu b\bar{b}$ analysis [11] are then combined to obtain a more precise measurement of the single top quark cross section and to place a lower limit on the CKM matrix element magnitude $|V_{tb}|$.

The CDF II detector is a multipurpose particle detector described in detail elsewhere [12]. It is comprised

of an inner silicon vertex detector, a 96-layer drift chamber spectrometer used for reconstructing charged-particle trajectories (tracks), and a calorimeter that is divided radially into electromagnetic and hadronic compartments, which are constructed of projective towers that cover pseudorapidities of up to $|\eta| < 3.6$ [13]. A system of drift chambers located outside the hadronic calorimeter is used for muon identification.

Jets are formed by clustering calorimeter energy deposits with an opening angle of $\Delta R \equiv \sqrt{(\Delta\eta)^2 + (\Delta\phi)^2} = 0.4$. Lepton candidates with large transverse momentum are identified by associating tracks with signatures in the appropriate detectors: energy deposits in the electromagnetic calorimeters for electrons, and muon-detector track segments for muons.

Events are selected in which the calorimeter missing transverse energy $\not\!\!E_T$(cal) satisfies a minimum online selection (trigger) threshold of at least 45 GeV, or 35 GeV if at least two jets are present. In the offline analysis, events are accepted if the reconstructed missing transverse energy $\not\!\!E_T$ is at least 35 GeV. A multivariate algorithm is used to parameterize the trigger efficiency as a function of several kinematic and angular variables of the event [14]. Measured jet energies are corrected to account for irregularities in calorimeter response, energy lost outside the jet cone, and underlying event dynamics [15]. The jet energy scale and resolution, as well as the $\not\!\!E_T$ resolution, are further improved by incorporating corrections based on charged-particle momentum measurements [16].

Each event is required to have at least two leading-E_T jets with transverse energies, $E_T^{j_1}$ and $E_T^{j_2}$, that satisfy $25 < E_T^{j_1} < 200$ GeV and $20 < E_T^{j_2} < 120$ GeV, respectively. Additionally, both leading-E_T jets are required to be reconstructed within the silicon detector acceptance, corresponding to pseudorapidity requirements of $|\eta| < 2$ for both jets, with one of them satisfying $|\eta| < 0.9$. Events with three jets are considered if the third-most energetic jet in E_T satisfies $15 < E_T^{j_3} < 100$ GeV and $|\eta| < 2.4$. Events with four or more jets are rejected if each jet satisfies the criteria $E_T > 15$ GeV and $|\eta| < 2.4$. To discriminate against MJ background, the angular separation between the two highest-E_T jets must satisfy $\Delta R > 0.8$. Events that satisfy these requirements are labeled "pre-tagged" events.

To suppress light-flavor MJ background, at least one of the leading-E_T jets is required to be b-tagged by the HOBIT algorithm [17], which assigns to each jet a value between 0 and 1. Jets with a HOBIT value between 0.72 (0.95) and 0.95 (1) are considered to be loosely (tightly) tagged. As two b quarks are present in the signal final state, events are separated into three categories based on the multiplicity and quality of the b-tagged jets: events with only one tightly tagged jet and no other tag (1T), events with two tightly tagged jets (TT), and events with one tightly tagged jet and one loosely tagged jet (TL). Events are further classified according to the total number of jets, leading to six event subsamples. Each subsample is analyzed separately to improve the sensitivity and to help separate the s- and t-channel produced events, which are enhanced in the double- and single-tagging categories, respectively.

All events that satisfy the above kinematic and b-tagging criteria are separated into two samples. Events that contain no identified leptons comprise the preselection sample, which includes events in the signal region, defined below. Events that contain at least one identified electron or muon comprise the electroweak sample, which is used to validate the background modeling derived for this analysis.

Most physics processes are modeled using Monte Carlo simulation programs. The single top quark samples are modeled using the POWHEG generator [18]. Backgrounds from V+jets (where V represents a W or Z boson) and $W + c$ processes are modeled using ALPGEN [19], with showering simulated by PYTHIA [20]. Events from diboson (VV), $t\bar{t}$ (assuming a top-quark mass of 172.5 GeV/c^2), and Higgs bosons produced in association with a W or Z boson (VH) are simulated using PYTHIA. Two remaining backgrounds include contributions from events with falsely tagged jets ("electroweak mistags") and MJ events.

The electroweak mistag samples are modeled by weighting V+jets and diboson-simulated events with mistag probabilities derived from dedicated data samples [21, 22]. To model the MJ background, the same data-driven method described in Ref. [23] is used: each pretagged data event is weighted by a tag-rate probability derived from a MJ-dominated data sample.

At this stage of the analysis, simple requirements on kinematic properties of the event are not sufficient to separate the single top quark signal from the background. A series of multivariate discriminants that take advantage of nontrivial variable correlations are therefore employed to optimize the suppression of MJ background and to separate the signal from the remaining backgrounds. For each of the multivariate algorithms described below, a combination of inputs is used corresponding to kinematic, angular, and event-topology quantities whose distributions are different between the background under consideration and the single top quark signal.

The dominant background in the preselection sample is MJ events. To discriminate against this background, the same $\mathrm{NN_{QCD}}$ multivariate discriminant that was developed in the $\not\!\!E_T b\bar{b}$ s-channel single top quark search [10] is used. All events that satisfy a minimum $\mathrm{NN_{QCD}}$ threshold requirement populate the signal region, in which the dominant backgrounds are from MJ production, V+heavy-flavor-jets events, and $t\bar{t}$ events. Events that do not meet the minimal $\mathrm{NN_{QCD}}$ threshold are used to validate the background prediction with the data. From this validation, multiplicative correction factors ranging from 0.7 to 0.9 are derived for each of the 1T,

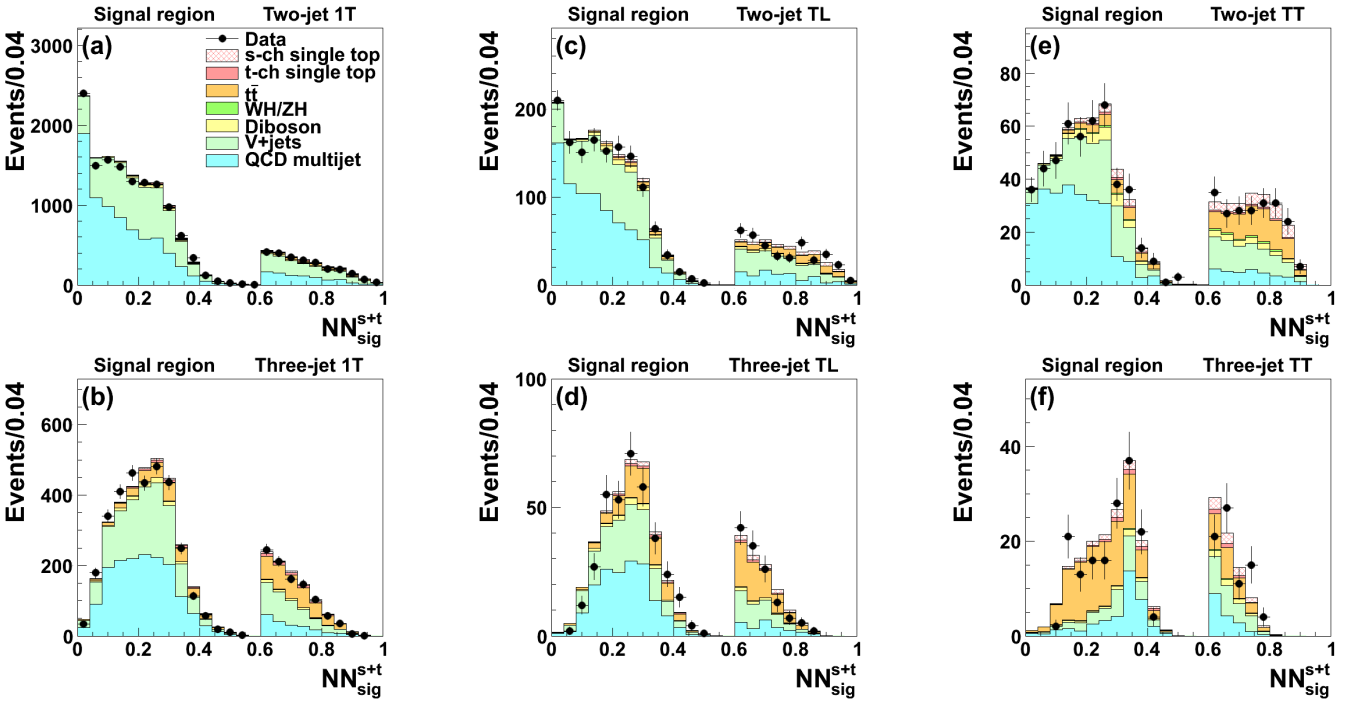

FIG. 1. Predicted and observed $\mathrm{NN}_{\mathrm{sig}}^{s+t}$ distributions in the signal region, for the (a) 1T two-jet, (b) 1T three-jet, (c) TL two-jet, (d) TL three-jet, (e) TT two-jet, (f) and TT three-jet subsamples.

TL and TT MJ predictions so that the total predicted background normalizations are in agreement with data. These corrections are applied to the MJ predictions in the signal region.

For all events in the signal region, two additional discriminants are developed that further exploit the differences in kinematic properties between the signal and the V+jets background, and the signal and $t\bar{t}$ background processes. The first discriminant $\mathrm{NN}_{V\mathrm{jets}}$ is trained using simulated t-channel single top quark events for the signal sample and MJ-modeled events that satisfy the requirement on $\mathrm{NN}_{\mathrm{QCD}}$, for the background sample. The second discriminant $\mathrm{NN}_{t\bar{t}}$ is trained to separate t-channel single top quark from $t\bar{t}$ production, again using simulated t-channel single top quark events for the signal but simulated $t\bar{t}$ for the background. The values of these two discriminants (both supporting values between 0 and 1) are then combined in quadrature for an overall discriminant called $\mathrm{NN}_{\mathrm{sig}}^{t}$; this is analogous to the strategy adopted to derive the final discriminant in the $\not\!\!E_T b\bar{b}$ s-channel single top quark search [10].

The s-channel optimized $\mathrm{NN}_{\mathrm{sig}}$ discriminant as used in the $\not\!\!E_T b\bar{b}$ s-channel single top quark search [10] and the $\mathrm{NN}_{\mathrm{sig}}^{t}$ discriminant of this analysis are combined to obtain an $\mathrm{NN}_{\mathrm{sig}}^{s+t}$ final discriminant, used to simultaneously separate both s- and t-channel signal processes from the remaining background. For events with $\mathrm{NN}_{\mathrm{sig}}$ output values larger than 0.6, $\mathrm{NN}_{\mathrm{sig}}^{s+t}$ is assigned to the $\mathrm{NN}_{\mathrm{sig}}$ output. For the remaining events, $\mathrm{NN}_{\mathrm{sig}}^{s+t}$ is defined as the $\mathrm{NN}_{\mathrm{sig}}^{t}$ output multiplied by 0.6. Figure 1 shows the predicted and observed distributions of the $\mathrm{NN}_{\mathrm{sig}}^{s+t}$ output variable for each of the six event subsamples used in this analysis.

Several sources of systematic uncertainty are taken into account. Uncertainties on assumed cross section values are included for $t\bar{t}$ (5%-6%), VV (6%), VH (5%), and $W+c$ (23%) processes [24–27]. Other systematic uncertainties arise from the normalization of the V-plus-heavy-flavor (30%) and of the MJ (3%-7%) background contributions. All samples whose normalizations are not constrained according to the data are subject to a luminosity uncertainty of 6% [28]. Furthermore, uncertainties are assigned due to the efficiencies of the lepton antiselection criteria (2%). We also assign a normalization uncertainty of 2% due to variations in the assumed parton distribution functions. To account for differences in the trigger efficiency in data and simulation, a 2% rate uncertainty is assigned.

Possible mismodeling in the b-tagging efficiency is taken into account by applying scale factors to the simulation to correct its b-tagging efficiency to that of data. All scale factors are determined from data control samples and are on the order of unity, with small variations depending on the tag category, and uncertainties ranging from 8% to 16% [17]. Mistag rate uncertainties (20%-30%) are also derived from data and included [17].

Uncertainties in the jet energy scale [15] are included by correlating the uncertainties in the predicted yields

of signals and backgrounds (of the order of 1%-6%) with the corresponding distortions in the predicted kinematic distributions arising from jet energy scale shifts in all samples except the MJ background, which is determined entirely from data. An additional systematic uncertainty is incorporated for the MJ model, accounting for shape variations in the MJ prediction.

To measure the signal cross section, a combined likelihood is formed, which is the product of Poisson probabilities for each bin of the six $\mathrm{NN}_{\mathrm{sig}}^{s+t}$ discriminants shown in Fig. 1. To account for systematic uncertainties, a Bayesian technique is used, in which each independent source of systematic uncertainty is assigned a nuisance parameter with a Gaussian prior probability density, truncated when necessary to ensure non-negative event yields. The impact of each nuisance parameter is propagated to the predictions of the signal and background yields in each bin of each histogram in the analysis. A non-negative uniform prior probability distribution is assumed for the single top quark cross section, which is extracted from its posterior probability density after integrating over all nuisance parameters.

Tables I and II show the event yields in the two- and three-jet subsamples, respectively, as determined from applying the measurement procedure to the six discriminants shown in Fig. 1. The observed single top quark production cross section ($\sigma_{\mathrm{obs}}^{s+t}$) is $3.53^{+1.25}_{-1.16}$ pb, consistent with the SM prediction of 3.15 ± 0.36 pb [5]. The magnitude of V_{tb} is extracted from the single top quark cross section posterior probability density by the relation $|V_{tb}|^2_{\mathrm{obs}} = |V_{tb}|^2_{\mathrm{SM}}\sigma^{s+t}_{\mathrm{obs}}/\sigma^{s+t}_{\mathrm{SM}}$, where variables with the subscript "SM" ("obs") correspond to the theoretical predictions (observed values) [29]. We assume $|V_{tb}|^2_{\mathrm{SM}}$ is unity and fix the s- and t-channel relative contributions to their SM prediction. Including the theoretical uncertainty of the signal cross section (5.8% for s-channel, 6.2% for t-channel) [5] and assuming a uniform prior in the interval $0 < |V_{tb}|^2 < 1$, a lower bound on $|V_{tb}|$ of 0.63 is obtained at the 95% credibility level (C.L.). We measure the t-channel cross section by itself to be $1.19^{+0.93}_{-0.97}$ pb, where the s-channel cross section is constrained to its SM prediction [30]; this result is consistent with the SM prediction of 2.10 ± 0.12 pb [5]. We also compute the two-dimensional posterior for the s- and t-channel cross sections, where the relative contributions of both channels are allowed to vary independently; the result is shown in Fig. 2a.

These results are combined with those of the most recent CDF measurement of single top quark production in the $\ell\nu b\bar{b}$ sample [11], which measured a cross section of $3.04^{+0.57}_{-0.53}$ pb assuming a top quark mass of 172.5 GeV/c^2. The combination is achieved by taking the product of the likelihoods of both analyses and simultaneously varying the correlated uncertainties, following the procedure explained above. In the $\ell\nu b\bar{b}$ analysis, candidate events were selected by requiring exactly one reconstructed charged lepton (e or μ) in the final state. Hence, no such events are included in the $\not\!\!E_T b\bar{b}$ analysis described above. The uncertainties associated with the theoretical cross sections of the $t\bar{t}$, VV, and VH production processes, and those associated with the luminosity are taken as fully correlated between the two analyses.

TABLE I. Numbers of predicted and observed events in the two-jet signal region in the subsamples with exactly one tightly tagged jet (1T), one tightly and one loosely tagged jet (TL), and two tightly tagged jets (TT). The uncertainties in the predicted numbers of events are due to the theoretical cross section uncertainties and to the uncertainties on signal and background modeling. Both the uncertainties and the central values are those determined by the fit to the data with theory constraints.

Category	1T	TL	TT
$t\bar{t}$	242.9 ± 24.3	84.8 ± 9.3	92.4 ± 8.4
VH	12.6 ± 1.4	6.6 ± 0.8	7.6 ± 0.8
Diboson	284.9 ± 25.6	51.3 ± 4.6	37.2 ± 3.4
V+jets	6527.7 ± 2048.1	694.2 ± 216.3	220.2 ± 68.7
MJ	8328.5 ± 180.6	885.2 ± 56.7	296.8 ± 31.8
s-ch single top	86.2 ± 47.7	41.8 ± 23.2	45.9 ± 25.3
t-ch single top	160.5 ± 30.8	10.8 ± 2.1	9.2 ± 1.7
Total prediction	15643.4 ± 2057.2	1774.8 ± 225.0	709.3 ± 80.3
Observed	15312	1743	686

TABLE II. Numbers of predicted and observed three-jet events in the 1T, TL, and TT subsamples.

Category	1T	TL	TT
$t\bar{t}$	596.5 ± 59.6	117.5 ± 12.8	109.5 ± 9.9
VH	6.0 ± 0.7	1.9 ± 0.2	2.2 ± 0.2
Diboson	107.7 ± 9.7	15.7 ± 1.5	8.8 ± 0.8
V+jets	1609.5 ± 505.1	164.5 ± 51.3	50.4 ± 15.8
MJ	1818.2 ± 48.7	187.5 ± 14.7	55.9 ± 7.7
s-ch single top	45.7 ± 25.3	15.4 ± 8.5	16.2 ± 8.9
t-ch single top	82.2 ± 15.8	7.5 ± 1.5	6.8 ± 1.3
Total prediction	4265.7 ± 511.9	510.0 ± 55.6	249.8 ± 22.1
Observed	4198	490	237

The combined measurement results in an electroweak single top quark production cross section of $3.02^{+0.49}_{-0.48}$ pb, consistent with the SM prediction. From the posterior probability density on $|V_{tb}|^2$, a 95% C.L. lower limit of $|V_{tb}| > 0.84$ is obtained. The t-channel cross section, measured in the same way as for the $\not\!\!E_T b\bar{b}$ analysis, is $1.65^{+0.38}_{-0.36}$ pb, in agreement with the SM prediction given above. The two-dimensional posterior probability is shown in Fig. 2b, where the relative s- and t-channel contributions are allowed to vary freely.

In summary, an updated measurement of the single top quark production cross section of $3.53^{+1.25}_{-1.16}$ pb is obtained in events with missing transverse energy and jets using the full CDF data set. This represents a relative improvement of 40% in overall precision with respect to the pre-

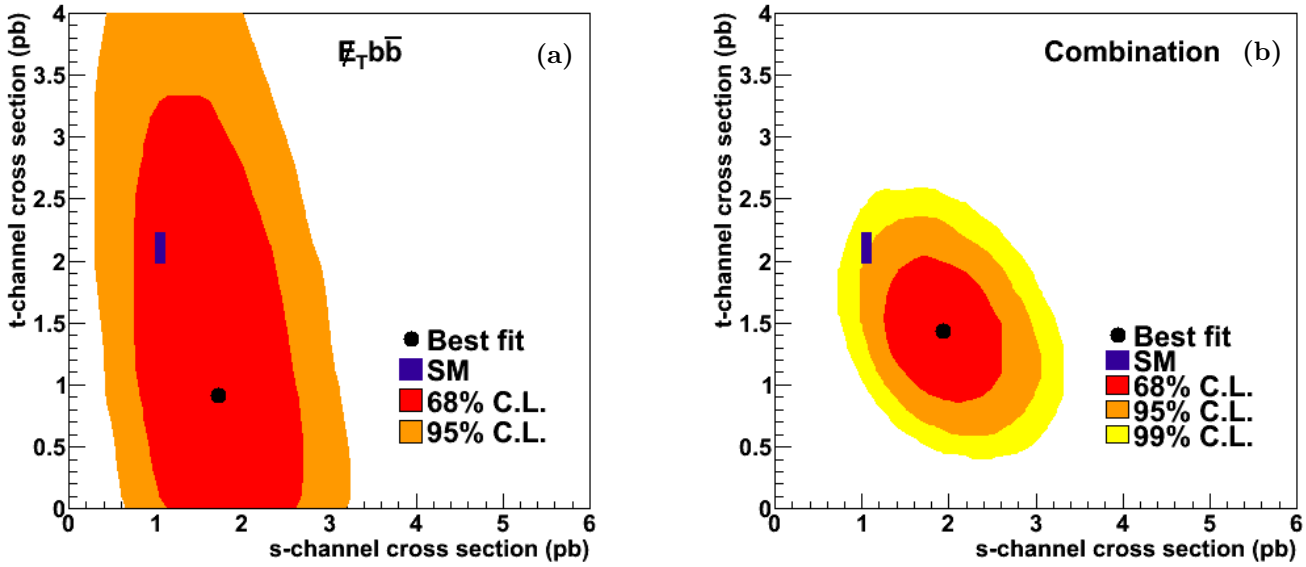

FIG. 2. Two-dimensional posterior probability densities of the s- and t-channel cross sections for the (a) $\not\!\!E_T b\bar{b}$ analysis presented here, and (b) the CDF combination of the $\not\!\!E_T b\bar{b}$ and $\ell\nu b\bar{b}$ analysis results. Theory uncertainties are not shown.

vious CDF analysis [9]. In addition, a combination with the $\ell\nu b\bar{b}$ CDF result [11] is performed to obtain a more precise cross section measurement of $3.04^{+0.57}_{-0.53}$ pb. Cross sections for the t-channel-only single top quark production process as well as 95% C.L. lower limits on $|V_{tb}|$ are also obtained for the $\not\!\!E_T b\bar{b}$ analysis and the CDF combination. All results are consistent with the corresponding SM predictions.

We thank the Fermilab staff and the technical staffs of the participating institutions for their vital contributions. This work was supported by the U.S. Department of Energy and National Science Foundation; the Italian Istituto Nazionale di Fisica Nucleare; the Ministry of Education, Culture, Sports, Science and Technology of Japan; the Natural Sciences and Engineering Research Council of Canada; the National Science Council of the Republic of China; the Swiss National Science Foundation; the A.P. Sloan Foundation; the Bundesministerium für Bildung und Forschung, Germany; the Korean World Class University Program, the National Research Foundation of Korea; the Science and Technology Facilities Council and the Royal Society, United Kingdom; the Russian Foundation for Basic Research; the Ministerio de Ciencia e Innovación, and Programa Consolider-Ingenio 2010, Spain; the Slovak R&D Agency; the Academy of Finland; the Australian Research Council (ARC); and the EU community Marie Curie Fellowship Contract No. 302103.

* Deceased
† With visitors from [a]University of British Columbia, Vancouver, BC V6T 1Z1, Canada, [b]Istituto Nazionale di Fisica Nucleare, Sezione di Cagliari, 09042 Monserrato (Cagliari), Italy, [c]University of California Irvine, Irvine, CA 92697, USA, [d]Institute of Physics, Academy of Sciences of the Czech Republic, 182 21, Czech Republic, [e]CERN, CH-1211 Geneva, Switzerland, [f]Cornell University, Ithaca, NY 14853, USA, [g]University of Cyprus, Nicosia CY-1678, Cyprus, [h]Office of Science, U.S. Department of Energy, Washington, DC 20585, USA, [i]University College Dublin, Dublin 4, Ireland, [j]ETH, 8092 Zürich, Switzerland, [k]University of Fukui, Fukui City, Fukui Prefecture, Japan 910-0017, [l]Universidad Iberoamericana, Lomas de Santa Fe, México, C.P. 01219, Distrito Federal, [m]University of Iowa, Iowa City, IA 52242, USA, [n]Kinki University, Higashi-Osaka City, Japan 577-8502, [o]Kansas State University, Manhattan, KS 66506, USA, [p]Brookhaven National Laboratory, Upton, NY 11973, USA, [q]Queen Mary, University of London, London, E1 4NS, United Kingdom, [r]University of Melbourne, Victoria 3010, Australia, [s]Muons, Inc., Batavia, IL 60510, USA, [t]Nagasaki Institute of Applied Science, Nagasaki 851-0193, Japan, [u]National Research Nuclear University, Moscow 115409, Russia, [v]Northwestern University, Evanston, IL 60208, USA, [w]University of Notre Dame, Notre Dame, IN 46556, USA, [x]Universidad de Oviedo, E-33007 Oviedo, Spain, [y]CNRS-IN2P3, Paris, F-75205 France, [z]Universidad Tecnica Federico Santa Maria, 110v Valparaiso, Chile, [aa]The University of Jordan, Amman 11942, Jordan, [bb]Universite catholique de Louvain, 1348 Louvain-La-

Neuve, Belgium, [cc]University of Zürich, 8006 Zürich, Switzerland, [dd]Massachusetts General Hospital, Boston, MA 02114 USA, [ee]Harvard Medical School, Boston, MA 02114 USA, [ff]Hampton University, Hampton, VA 23668, USA, [gg]Los Alamos National Laboratory, Los Alamos, NM 87544, USA, [hh]Università degli Studi di Napoli Federico I, I-80138 Napoli, Italy

[1] V. M. Abazov *et al.* (D0 Collaboration), Phys. Rev. Lett. **103**, 092001 (2009); T. Aaltonen *et al.* (CDF Collaboration), Phys. Rev. Lett. **103**, 092002 (2009).

[2] N. Cabibbo, Phys. Rev. Lett. **10**, 531 (1963); M. Kobayashi and T. Maskawa, Prog. Theor. Phys. **49**, 652 (1973).

[3] Charge-conjugate processes are assumed throughout unless explicitly stated otherwise.

[4] N. Kidonakis, Phys. Rev. D **74**, 114012 (2006).

[5] N. Kidonakis, Phys. Rev. D **81**, 054028 (2010); **83**, 091503(R) (2011).

[6] This value assumes equal contributions from singly produced top and antitop quarks.

[7] We assume a branching ratio of 100% for the standard-model $t \to W^+ b$ process.

[8] The calorimeter missing transverse energy $\vec{\not\!\!E}_T$(cal) is defined by the sum over calorimeter towers, $\vec{\not\!\!E}_T(\text{cal}) = -\sum_i E_T^i \hat{n}_i$, where i is a calorimeter tower number with $|\eta| < 3.6$, and $\hat{n}_i$ is a unit vector perpendicular to the beam axis and pointing at the ith calorimeter tower. The reconstructed missing transverse energy, $\vec{\not\!\!E}_T$, is derived by subtracting from $\vec{\not\!\!E}_T$(cal) components of the event not registered by the calorimeter, such as jet energy adjustments. $\not\!\!E_T$ [$\not\!\!E_T$(cal)] is the scalar magnitude of $\vec{\not\!\!E}_T$ [$\vec{\not\!\!E}_T$(cal)].

[9] T. Aaltonen *et al.* (CDF Collaboration), Phys. Rev. D **81**, 072003 (2010).

[10] T. Aaltonen *et al.* (CDF Collaboration), Phys. Rev. Lett. **112**, 231805 (2014).

[11] T. Aaltonen *et al.* (CDF Collaboration), Phys. Rev. Lett., to be published, `arXiv:1407.4031 [hep-ex]`.

[12] D. Acosta *et al.* (CDF Collaboration), Phys. Rev. D **71**, 032001 (2005); **71**, 052003 (2005); A. Abulencia *et al.*, (CDF Collaboration) J. Phys. G **34**, 2457 (2007).

[13] We use a cylindrical coordinate system where θ is the polar angle relative to the proton beam direction at the event vertex, ϕ is the azimuthal angle about the beam axis, and pseudorapidity is defined $\eta = -\ln\tan(\theta/2)$. We define transverse energy as $E_T = E\sin\theta$ and transverse momentum as $p_T = p\sin\theta$ where E is the energy measured in the calorimeter and p is the magnitude of the momentum measured by the spectrometer.

[14] K. Potamianos, Ph.D. thesis, Purdue University [FERMILAB-THESIS-2011-34, 2011].

[15] A. Bhatti *et al.*, Nucl. Instrum. Methods A **566**, 375 (2006).

[16] C. Adloff *et al.* (H1 collaboration), Z. Phys. C **74**, 221 (1997).

[17] J. Freeman, T. Junk, M. Kirby, Y. Oksuzian, T. J. Phillips, F. D. Snider, M. Trovato, J. Vizan, and W. M. Yao, Nucl. Instrum. Methods Phys. Res., Sect. A **697**, 64 (2013).

[18] S. Alioli, P. Nason, C. Oleari, and E. Re, J. High Energy Phys. 06 (2010) 043.

[19] M. L. Mangano, M. Moretti, F. Piccinini, R. Pittau, and A. D. Polosa, J. High Energy Phys. 07 (2003) 001.

[20] T. Sjöstrand, S. Mrenna, and P. Skands, J. High Energy Phys. 05 (2006) 026.

[21] D. Acosta *et al.* (CDF Collaboration), Phys. Rev. D **71**, 052003 (2005).

[22] A. Abulencia *et al.* (CDF Collaboration), Phys. Rev. D **74**, 072006 (2006).

[23] T. Aaltonen *et al.* (CDF Collaboration), Phys. Rev. D **87**, 052008 (2013).

[24] P. Bärnreuther, M. Czakon, and A. Mitov, Phys. Rev. Lett. **109**, 132001 (2012).

[25] J. M. Campbell and R. K. Ellis, Phys. Rev. D **60**, 113006 (1999).

[26] J. Baglio and A. Djouadi, J. High Energy Phys. 10 (2010) 064; O. Brien, R. V. Harlander, M. Weisemann, and T. Zirke, Eur. Phys. J. C **72**, 1868 (2012).

[27] T. Aaltonen *et al.* (CDF Collaboration), Phys. Rev. Lett. **110**, 071801 (2013).

[28] S. Klimenko, J. Konigsberg, and T. M. Liss, Report No. FERMILAB-FN-0741 (2003).

[29] This relation is robust assuming that $|V_{tb}|^2 \gg |V_{ts}|^2 + |V_{td}|^2$.

[30] This Letter does not report a separate s-channel cross section result, which is presented in Ref. [10].